Nonreciprocal single-photon quantum router

Ya-long Ren,[1] Sheng-li Ma,[1,*] Ji-kun Xie,[1] Xin-ke Li,[1] Ming-tao Cao,[2,†] and Fu-li Li[1]

[1]*MOE Key Laboratory for Nonequilibrium Synthesis and Modulation of Condensed Matter, Shaanxi Province Key Laboratory of Quantum Information and Quantum Optoelectronic Devices, School of Physics, Xi'an Jiaotong University, Xi'an 710049, China*

[2]*Key Laboratory of Time and Frequency Primary Standards, National Time Service Center, Chinese Academy of Sciences, Xi'an 710600, China*

(Received 20 September 2021; accepted 24 December 2021; published 14 January 2022)

The quantum router is an elementary building block in quantum information processing and quantum communication. This work constitutes a step forward in this direction, i.e., an efficient scheme is proposed for the implementation of a nonreciprocal single-photon quantum router, allowing the routing of a single photon from one side but blocking it from the other side. Our model consists of two directly coupled coplanar-waveguide resonators and a superconducting ring resonator, which are connected together through a transmission line. The nonreciprocity is realized by unidirectionally interacting the rotating microwave modes of the ring resonator with a dissipative magnon mode in an yttrium iron garnet disk. We find that a single-photon signal can be delivered from a given input port to either of the two output ports, but is fully absorbed from the opposite one. The proposed scheme not only enriches the family of nonreciprocal quantum devices, but also finds useful applications in chiral quantum technologies.

DOI: 10.1103/PhysRevA.105.013711

I. INTRODUCTION

Building a quantum network [1,2] enables important applications, such as quantum-enhanced computing [3,4], advanced simulation [5,6], secure communication [7–9], and distributed sensing [10]. Basically, a quantum network is composed of a series of channels and nodes [11–15], including quantum amplifier [16], isolator [17–19], frequency converter [20–22], quantum router [23–26], and so on [27–30]. Among them, the quantum router is an essential element, and can be exploited to direct signals from its source to different quantum channels. So the quantum router has attracted wide interests in recent years, and great progress on this subject has been made by using the coupled resonator-waveguide systems [31–33], cavity optomechanical systems [34–36], and atomic systems [25,37–42].

In parallel, the nonreciprocal optical devices, which break the Lorentz reciprocity of light [43], are indispensable for a variety of practical applications, such as communication technologies [44], sensing [45–47], and optical signal processing [48,49]. The incident light displays different physical phenomena when it propagates along with the different directions in these nonreciprocal devices. On one hand, the nonreciprocal transmission of classical fields have been experimentally demonstrated with optical nonlinearity [50–57], spatiotemporal modulation of permittivity [58,59], chiral optics [60], synthetic materials [61,62], atoms [63–66], and spinning cavities [67]. On the other hand, there also has been a large number of research works for developing nonreciprocal quantum devices, such as control of thermal noise [68], one-way photon blockade [69] and quantum amplifier [70,71], single-photon diodes [72–75], and nonreciprocal entanglement [76]. These devices are fundamental elements in chiral quantum technologies.

In this work, we present a theoretical framework for the realization of a nonreciprocal single-photon quantum router. Our model is based on a cascaded quantum system that consists of two linearly coupled coplanar-waveguide (CPW) resonators and a superconducting ring resonator. The CPW and ring resonators are interconnected together through a transmission line. In addtion, an yttrium iron garnet (YIG) disk is placed on top of the ring resonator that supports both the counterclockwise (CCW) and the clockwise (CW) rotating microwave modes [77–81]. Owing to the selective coupling rule, the magnon mode in YIG can only couple to the rotating microwave modes with the same chirality [78–80]. As a result, the time-reversal symmetry is broken and the nonreciprocity can be realized. For a given direction, an input single photon is decoupled from the magnon mode. We show that the two coupled CPW resonators act in the role of a quantum router that can deliver the left-input photon to either of the two output ports. On the contrary, an incident single photon from the right direction is strongly affected by the magnon mode with a large decay rate, and can be completely absorbed. This perfect photon-absorption phenomenon can be interpreted as the appearance of a sharp symmetry-breaking transition in a parity-time (PT)-symmetric Hamiltonian with the balanced gain and loss [82–84]. Thus we design a one-way quantum device to route the single photon nonreciprocally, which can protect the signal resource against the undesired signals from the opposite direction. The present work not only enriches the family of nonreciprocal devices, but also finds a wide range of practical applications, such as the noise-tolerant quantum information processing [85,86] and the chiral quantum network [87–89].

*msl1987@xjtu.edu.cn
†mingtaocao@ntsc.ac.cn

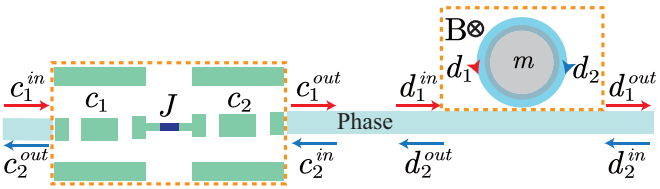

FIG. 1. Nonreciprocal single-photon quantum router based on circuit QED implementation. Two coupled superconducting CPW resonators and a superconducting ring resonator are linked together through a transmission line. A YIG disk (gray color) is placed on top of the ring resonator and biased perpendicularly by an external static magnetic field B.

II. THEORETICAL MODEL

A. Hamiltonian

As depicted in Fig. 1, we consider a circuit QED architecture where two quantum nodes are interconnected through a one-dimensional transmission line. The first node is composed of two directly coupled CPW resonators. The CPW resonator can be modeled as the simple harmonic oscillators, where two ground planes are placed on the two sides of a narrow central conductor [90]. By just considering the fundamental cavity mode, we first give the Hamiltonian of the two coupled CPW resonators (hereafter $\hbar = 1$)

$$H_1 = \omega_c(c_1^\dagger c_1 + c_2^\dagger c_2) + J(c_1^\dagger c_2 + c_1 c_2^\dagger), \tag{1}$$

where c_1 and c_2 are the annihilation operators of two CPW resonators with identical frequency ω_c. J represents the photon hopping rate, and can be experimentally implemented by connecting the independent resonators via a coupler, such as a superconducting quantum interference device [91,92]. Additionally, the parameter J can be tuned dynamically by adjusting the effective inductance of the coupler [93].

The second node is formed by a superconducting ring resonator coupled to a single YIG disk. Because of the symmetry of the geometric structure, the ring resonator inherently possesses a degenerate pair of propagating microwave modes, i.e., CW and CCW modes [77–81]. When an external static magnetic field B is applied, the YIG disk is uniformly magnetized and supports various magnon modes [94–97]. Here we only focus on the kittel mode, and the associated Hamiltonian reads

$$\begin{aligned} H_2 =& \omega_m m^\dagger m + \omega_d(d_1^\dagger d_1 + d_2^\dagger d_2) \\ &+ G_1(d_1^\dagger m + d_1 m^\dagger) + G(d_2^\dagger m + d_2 m^\dagger), \end{aligned} \tag{2}$$

where d_1 (d_2) is the annihilation operator for the CCW (CW) microwave mode with the resonance frequency ω_d. m is the annihilation operator of the magnon mode with the resonance frequency $\omega_m = \gamma B$, where $\gamma/2\pi = 28\,\mathrm{GHz/T}$ is the gyromagnetic ratio. In addition, G_1 (G) describes the coupling strength between the CCW (CW) microwave mode and the magnon mode. It has turned out that the magnon mode only couples to one of the propagating modes with the same chirality [78–80]. As a result, the perfect chiral coupling can be realized, where we have $G_1 = 0$ and $G \neq 0$. Since the magnon mode is decoupled from the d_1 mode, the time-reversal symmetry is broken, leading to the nonreciprocal single-photon transmission.

At present, the total Hamiltonian describing the system takes the form

$$\begin{aligned} H =& \omega_c(c_1^\dagger c_1 + c_2^\dagger c_2) + \omega_d(d_1^\dagger d_1 + d_2^\dagger d_2) + \omega_m m^\dagger m \\ &+ J(c_1^\dagger c_2 + c_1 c_2^\dagger) + G(d_2^\dagger m + d_2 m^\dagger). \end{aligned} \tag{3}$$

B. Output spectrum

We now derive the output spectrums of the left-input and right-input photons. According to Hamiltonian (3), the quantum Langevin equations (QLEs) of the system are given by

$$\begin{aligned} \dot{c}_1 &= -(i\omega_c + \kappa_c + \Gamma_c)c_1 - iJc_2 + \sqrt{2\kappa_c}c_1^{\mathrm{in}}, \\ \dot{c}_2 &= -(i\omega_c + \kappa_c + \Gamma_c)c_2 - iJc_1 + \sqrt{2\kappa_c}c_2^{\mathrm{in}}, \\ \dot{d}_1 &= -(i\omega_d + \kappa_d + \Gamma_d)d_1 + \sqrt{2\kappa_d}d_1^{\mathrm{in}}, \\ \dot{d}_2 &= -(i\omega_d + \kappa_d + \Gamma_d)d_2 - iGm + \sqrt{2\kappa_d}d_2^{\mathrm{in}}, \\ \dot{m} &= -(i\omega_m + \gamma_m)m - iGd_2. \end{aligned} \tag{4}$$

In the above equation, we dropped the quantum noise operators whose contributions to the output spectrums can be neglected when the system is operated at a low temperature. At the working temperature 20 mK, the average thermal excitation of each mode is about 10^{-7} for the resonance frequency $2\pi \times 6\,\mathrm{GHz}$. κ_c, κ_d capture the external damping rates and are related to the coupling of the transmission line to the superconducting resonators. Γ_c, Γ_d, and γ_m are the intrinsic damping rates. c_1^{in} (d_1^{in}) and c_2^{in} (d_2^{in}) describe the input signals that are coming from the left (right) side of the transmission line.

By introducing the Fourier transform $f(t) = \int_{-\infty}^{+\infty} \frac{d\omega}{2\pi} f(\omega)e^{-i\omega t}$, we can rewrite Eq. (4) in the frequency domain as

$$\begin{aligned} (i\Delta_c + \kappa_c + \Gamma_c)c_1(\omega) + iJc_2(\omega) &= \sqrt{2\kappa_c}c_1^{\mathrm{in}}(\omega), \\ (i\Delta_c + \kappa_c + \Gamma_c)c_2(\omega) + iJc_1(\omega) &= \sqrt{2\kappa_c}c_2^{\mathrm{in}}(\omega), \\ (i\Delta_d + \kappa_d + \Gamma_d)d_1(\omega) &= \sqrt{2\kappa_d}d_1^{\mathrm{in}}(\omega), \\ (i\Delta_d + \kappa_d + \Gamma_d)d_2(\omega) + iGm(\omega) &= \sqrt{2\kappa_d}d_2^{\mathrm{in}}(\omega), \\ (i\Delta_m + \gamma_m)m(\omega) + iGd_2(\omega) &= 0, \end{aligned} \tag{5}$$

where $\Delta_c = \omega_c - \omega$, $\Delta_d = \omega_d - \omega$, and $\Delta_m = \omega_m - \omega$ are the detunings. We stress here that the frequency bandwidth of the transmission line is much larger than the total damping rate of the resonator. Hence the transmission line can be regarded as a Markovian reservoir [97]. Under this premise, we can exploit the standard input-output boundary conditions $d_1^{\mathrm{out}}(\omega) = d_1^{\mathrm{in}}(\omega) - \sqrt{2\kappa_d}d_1(\omega)$, $d_1^{\mathrm{in}}(\omega) = e^{i\varphi}c_1^{\mathrm{out}}(\omega)$, $c_1^{\mathrm{out}}(\omega) = c_2^{\mathrm{in}}(\omega) - \sqrt{2\kappa_c}c_2(\omega)$, $c_2^{\mathrm{in}}(\omega) = e^{i\varphi}d_2^{\mathrm{out}}(\omega)$, $d_2^{\mathrm{out}}(\omega) = d_2^{\mathrm{in}}(\omega) - \sqrt{2\kappa_d}d_2(\omega)$, and $c_2^{\mathrm{out}}(\omega) = c_1^{\mathrm{in}}(\omega) - \sqrt{2\kappa_c}c_1(\omega)$. Here φ is the phase accumulated by the photon traveling in the transmission line, determined by the separation distance between the CPW resonator and the ring resonator. Then, the output fields can be readily derived as

$$U_{\mathrm{out}}(\omega) = S(\omega)U_{\mathrm{in}}(\omega). \tag{6}$$

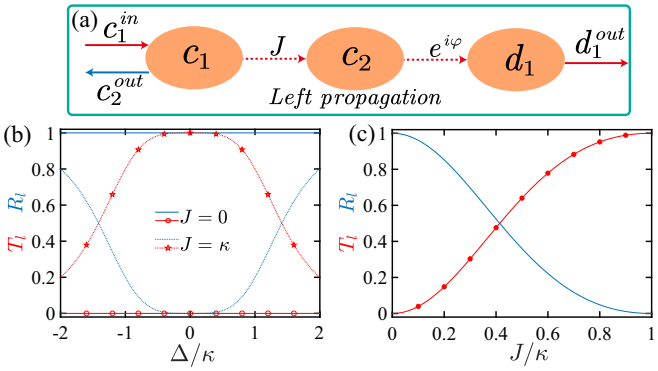

FIG. 2. (a) Scattering diagram of the left-incident photon. (b) Transmission T_l and reflection R_l spectrums as a function of the detuning Δ/κ for different J. (c) Transmission T_l and reflection R_l spectrums versus the hopping rate J/κ with $\Delta = 0$. We set $\Gamma = 0$.

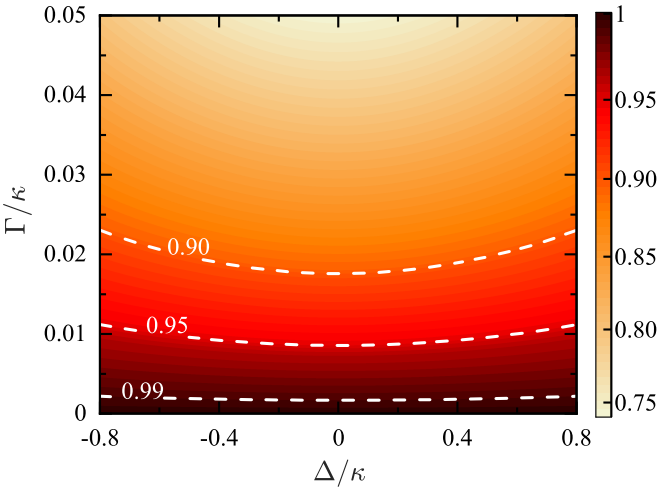

FIG. 3. Left-going photon: Total spectrum S_l versus the intrinsic damping rate Γ/κ and the detuning Δ/κ, where we set $J = \kappa$.

In Eq. (6), $U_{\rm in}(\omega) = [c_1^{\rm in}(\omega), d_2^{\rm in}(\omega)]^T$ and $U_{\rm out}(\omega) = [d_1^{\rm out}(\omega), c_2^{\rm out}(\omega)]^T$ are the vectors of the input and output fields, respectively; $S(\omega)$ is the scattering matrix

$$S(\omega) = \begin{pmatrix} t_{cd} & r_{dd} \\ r_{cc} & t_{dc} \end{pmatrix}, \tag{7}$$

where the relevant matrix elements are given by

$$\begin{aligned} t_{cd} &= i\frac{2J\kappa_c}{[i\Delta_c + (\kappa_c + \Gamma_c)]^2 + J^2} De^{i\varphi}, \\ r_{cc} &= \frac{[i\Delta_c + (\kappa_c + \Gamma_c)][i\Delta_c - (\kappa_c - \Gamma_c)] + J^2}{[i\Delta_c + (\kappa_c + \Gamma_c)]^2 + J^2}, \\ t_{dc} &= t_{cd}M/D,\ r_{dd} = r_{cc}MDe^{i2\varphi} \end{aligned} \tag{8}$$

with $M = \frac{(i\Delta_m+\gamma_m)[i\Delta_d-(\kappa_d-\Gamma_d)]+G^2}{(i\Delta_m+\gamma_m)[i\Delta_d+(\kappa_d+\Gamma_d)]+G^2}$ and $D = \frac{i\Delta_d-(\kappa_d-\Gamma_d)}{i\Delta_d+(\kappa_d+\Gamma_d)}$. The matrix elements in Eq. (7) determine the scattering behavior of an input single-photon state. Owing to the unidirectional magnon-photon coupling, the scattering matrix is asymmetric. Consequently, the system will manifest different physical responses with respect to the input directions of the single photon. By tuning the system's parameters, we can route the left-going photon on-demand, and fully block the right-going photon. To facilitate our discussion, we set $\omega_c = \omega_d = \omega_m = \omega_0$, $\Delta_c = \Delta_d = \Delta_m = \Delta$, $\kappa_c = \kappa_d = \kappa$, and $\Gamma_c = \Gamma_d = \Gamma$ in subsequent sections.

III. NONRECIPROCAL SINGLE-PHOTON ROUTER

A. Left-going photon

First, let us investigate the physical response of the system when the incident photon is injected from the left side of the transmission line, i.e., $c_1^{\rm in} \neq 0$ and $d_2^{\rm in} = 0$. In this case, the output fields yield $d_1^{\rm out} = t_{cd}c_1^{\rm in}$ and $c_2^{\rm out} = r_{cc}c_1^{\rm in}$. Figure 2(a) intuitively displays the coherent scattering behavior of the left-input photon. Note that the ring resonator in this direction is decoupled from the magnon mode, so the left-input photon passes through it without reflection. As a result, the two coupled CPW resonators play the role of a quantum router, dominating the transmission manner of the left-input photon. When a single photon is fed into the two CPW resonators from the left side, it can be transmitted or reflected, controlled by the hopping rate J. We now discuss the mechanism of routing the left-input photon. For $J = 0$, the first CPW resonator is side-coupled to a superconducting transmission line. The system can be regarded as a complete reflector, so that an incoming photon is fully reflected. For $J = \kappa$, the quantum critical coupling condition can be achieved [98], which involves the intricate balance between the inter-resonator coupling and the resonator-waveguide couplings. Hence, the system acts as a complete lens and the single photon is totally transmitted. For $J \in [0, \kappa]$, the transport of the left-incident photon can be tuned on-demand with an arbitrary ratio.

To elucidate the above discussion, we numerically simulate the transmission probability $T_l = |t_{cd}|^2$ and the reflection probability $R_l = |r_{cc}|^2$ by changing the parameter J. It is observed from Fig. 2(b) that, around the central resonance frequency $\Delta = 0$, we have the transmission coefficient $T_l = 0$ and reflection coefficient $R_l = 1$ for $J = 0$; while the coefficients $T_l = 1$ and $R_l = 0$ are obtained for $J = \kappa$. Moreover, we also plot the transmission and reflection spectrums for $J \in [0, \kappa]$ in Fig. 2(c). As expected, the transmission (reflection) probability can be continuously tuned from 0 (1) to 1 (0) by changing the hopping rate J from 0 to κ. Thus, the efficient routing of the left-input photon is realized.

In the practical situation, the intrinsic photonic losses of the microwave resonators are inevitable to affect the routing performance. To analyze their influence, we introduce the total spectrum $S_l = T_l + R_l$ (we have $S_l = 1$ for the ideal case $\Gamma = 0$). As shown in Fig. 3, the total spectrum S_l gradually decreases with the increase of the intrinsic decay rate Γ. However, the routing capability is still sufficient enough under a relatively small Γ. For $\Gamma/\kappa < 0.0017$, the total spectrum $S_l > 0.99$ can be achieved over a large frequency range, which means that a nearly perfect single-photon router can be implemented. If we set $\kappa/2\pi = 20\,\text{MHz}$, the intrinsic decay rate $\Gamma/2\pi < 34\,\text{kHz}$ is required to reach $S_l > 0.99$, and the needed internal quality factor is $Q_i = \omega_0/\Gamma > 1.8 \times 10^5$ for a cavity frequency $\omega_0/2\pi = 6\,\text{GHz}$. Experimentally, the internal quality factor $Q_i > 10^7$ of the superconducting

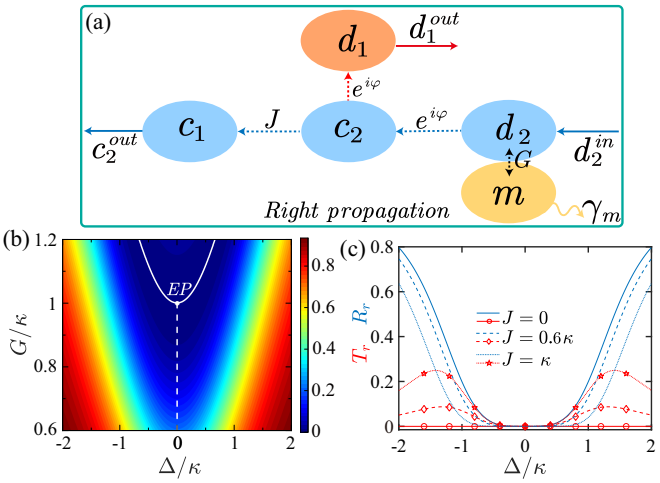

FIG. 4. (a) Scattering diagram of the right-incident photon. (b) Total spectrum S_r as a function of the coupling strength G/κ and the detuning Δ/κ with $J=\kappa$. (c) Transmission T_r and reflection R_r versus the detuning Δ/κ for different J. We set $G=\gamma_m=\kappa$ and $\Gamma=0$.

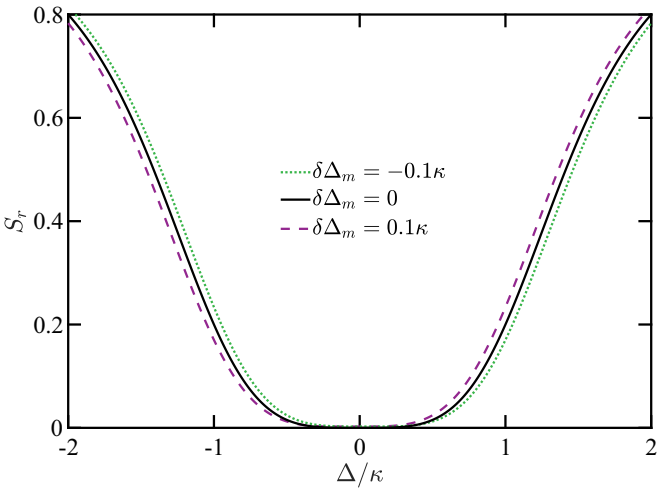

FIG. 5. Total spectrum S_r as a function of Δ/κ for different $\delta\Delta_m$. We set $G=\gamma_m=\kappa=J$ and $\Gamma=0$.

cavities has been reported [99,100]. Therefore, the quantum routing scheme is applicable to the currently available technologies.

B. Right-going photon

Second, we study the scatting behavior of an incident photon coming from the right side of the transmission line. As illustrated in Fig. 4(a), the output of the right-going photon is given by $d_1^{\rm out}=r_{dd}d_2^{\rm in}$ and $c_2^{\rm out}=t_{dc}d_2^{\rm in}$. Here, we label $T_r=|t_{dc}|^2$ and $R_r=|r_{dd}|^2$ as the transmission and reflection probabilities. If the condition $G=\gamma_m=\kappa-\Gamma$ is satisfied, we can get $T_r=R_r=0$ at the point $\Delta=0$ from Eq. (8). This suggests that the right-propagating photon is completely absorbed, which refers to a phase transition in a PT-symmetric Hamiltonian of the coupled magnon-photon system. The signal photon is totally dissipated into the environment through the intrinsic loss of the magnon mode.

We now detail the mechanism of the perfect single-photon absorption. Provided that the right-input photon has zero output $d_1^{\rm out}=c_2^{\rm out}=0$, we can derive $d_2^{\rm in}=\sqrt{2\kappa_d}d_2$ from the input-output relation. So the reduced QLEs in Eq. (4) can be obtained

$$\begin{aligned}\dot{d}_2&=-(i\omega_0-\kappa_e)d_2-iGm,\\ \dot{m}&=-(i\omega_0+\gamma_m)m-iGd_2,\end{aligned}\tag{9}$$

with $\kappa_e=\kappa-\Gamma$. Thus the dynamics of d_2 and m is dominated by a non-Hermitian Hamiltonian $H_e=(\omega_0+i\kappa_e)d_2^\dagger d_2+(\omega_0-i\gamma_m)m^\dagger m$; that is,

$$H_e=\begin{pmatrix}\omega_0+i\kappa_e & G\\ G & \omega_0-i\gamma_m\end{pmatrix}.\tag{10}$$

For $\kappa_e>0$, the right-input photon corresponds to an effective gain for the mode d_2. When the condition $\kappa_e=\gamma_m$ is satisfied, H_e becomes a standard PT-symmetric Hamiltonian with $[PT,H_e]=0$ [101] whose eigenfrequencies are given by

$$\lambda_\pm=\omega_0\pm\sqrt{G^2-\gamma_m^2}.\tag{11}$$

In the PT-symmetric-broken region $G<\gamma_m$, the eigenfrequencies $\lambda_\pm$ are a complex conjugate pair. In the PT-symmetric region $G>\gamma_m$, the eigenfrequencies $\lambda_\pm$ become real values. For $G=\gamma_m$, a sharp transition occurs from the PT-symmetry-breaking phase to the PT-symmetric phase, and the eigenfrequencies $\lambda_\pm$ coalesce. This corresponds to the non-Hermitian parameter crossing an exceptional point with the balanced gain and loss [82–84]. So, when the condition $G=\gamma_m=\kappa-\Gamma$ is satisfied, the coupled magnon-photon system is operated at the exceptional point. The right-input photon will be completely transferred from the microwave mode d_2 to the dissipative magnon mode m, giving rise to the perfect photon absorption. Figure 4(b) displays the output spectrum $S_r=T_r+R_r$ of the right-incident photon. We can observe that $S_r=0$ is confirmed at the exceptional point. Moreover, since the right-input photon cannot be transported to the CPW resonators at the exceptional point, the hopping rate J does not affect the output spectrum S_r, as illustrated in Fig. 4(c).

In the above discussion we assumed that ω_m is equal to the other resonance frequencies. Due to the fluctuation of external magnetic field B, a frequency shift $\delta\Delta_m$ ($\Delta_m=\Delta+\delta\Delta_m$) can be induced, affecting the absorption of the right-input photon. However, our scheme has a large isolation bandwidth $\sim\kappa$ for the right-input photon, as shown in Fig. 4(c). Hence its effect on the photon absorption is negligible for the case $\delta\Delta_m\ll\kappa$, which can be demonstrated in Fig. 5.

C. Nonreciprocity

We discussed the different scattering behaviors of the left-going and right-going photons. To quantitatively describe the nonreciprocity of the proposed one-way quantum router, we introduce the contrast ratio $\eta=|(S_l-S_r)/(S_l+S_r)|$. As shown in Fig. 6, we plot the contrast ratio η as a function of the hopping rate J/κ and the detuning Δ/κ. Remarkably, the

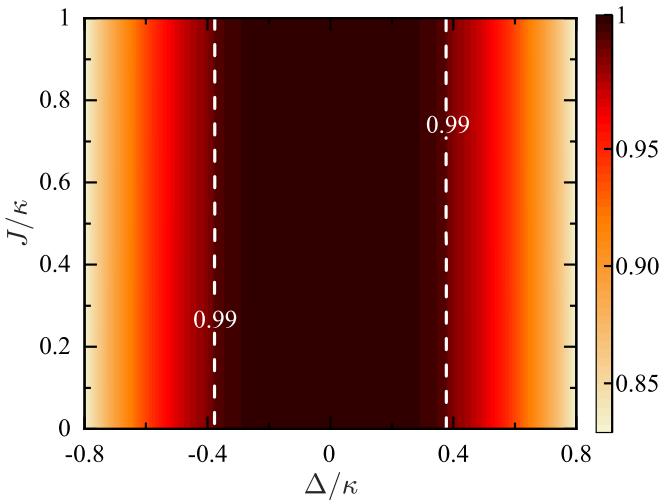

FIG. 6. The contrast ratio η as a function of the hopping rate J/κ and the detuning Δ/κ, where we set $G = \gamma_m = \kappa$ and $\Gamma = 0$.

numerical results demonstrate that the isolation performance works well in a large operational bandwidth $\sim 0.8\kappa$, where the nonreciprocal single-photon router can be performed with a contrast ratio larger than 0.99.

Up to now, the proposed nonreciprocal single-photon quantum router is built on the ideal chiral coupling $G_1 = 0$ and $G \neq 0$. However, the condition $G_1 = 0$ may not be satisfied in a realistic device, i.e., there exists a direct coupling between the magnon mode m and the CCW microwave mode d_1. So the presence of G_1 will lead to the signal loss of the left-input photon, as well as the signal transmission of the right-input photon. This degrades the quality of the nonreciprocal quantum router. In Fig. 7, we investigate the effect of G_1 on the total spectrums and the contrast ratio. For $G_1 \in [0, 0.1G]$, the left-going photon almost has no loss with $S_l > 0.99$, and the right-going photon can be almost completely absorbed with $S_r < 0.01$. Additionally, the contrast ratio $\eta > 0.99$ can be obtained for $G_1 < 0.07G$. Therefore, we should keep $G_1 < 0.07G$ for guaranteeing a high-performance nonreciprocal quantum router.

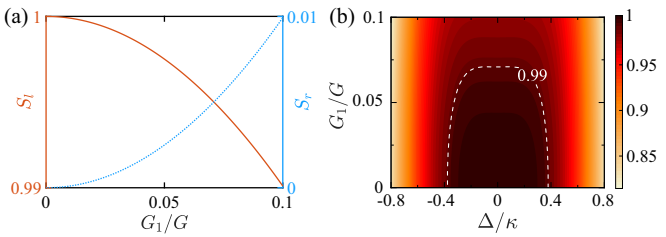

FIG. 7. (a) Total spectrums S_l (solid line) and S_r (dotted line) as a function of the coupling strength G_1/G for $\Delta = 0$. (b) The contrast ratio η as a function of the coupling strength G_1/G and the detuning Δ/κ. We set $G = \gamma_m = \kappa = J$ and $\Gamma = 0$.

IV. CONCLUSION

In conclusion, we proposed a method to generate a nonreciprocal single-photon quantum router in a composite system of superconducting resonators and a YIG disk. The nonreciprocity arises from the selective coupling between the magnon mode and the propagating microwave modes with the same chirality. We show that an input photon from the left side of the transmission line can be routed to one of the two output channels. While an input photon from the right side of the transmission line can be completely absorbed by the dissipative magnon mode, which is related to a phase transition in a non-Hermitian PT-symmetric Hamiltonian with the balanced gain and loss. The proposed nonreciprocal device can protect the signal source from extraneous noise and has beneficial applications in the fields of quantum computation and quantum network.

ACKNOWLEDGMENTS

This work was supported by the National Natural Science Foundation of China (Grants No. 11704306 and No. 12074307) and the Fundamental Research Funds for the Central Universities (Grant No. 11913291000022).

[1] H. J. Kimble, Nature (London) **453**, 1023 (2008).
[2] S. Wehner, D. Elkouss, and R. Hanson, Science **362**, eaam9288 (2018).
[3] F. Arute *et al.*, Nature (London) **574**, 505 (2019).
[4] H.-S. Zhong *et al.*, Science **370**, 1460 (2020).
[5] E. Rico, T. Pichler, M. Dalmonte, P. Zoller, and S. Montangero, Phys. Rev. Lett. **112**, 201601 (2014).
[6] M. Gong *et al.*, Science **372**, 948 (2021).
[7] B. Fröhlich, J. F. Dynes, M. Lucamarini, A. W. Sharpe, Z. Yuan, and A. J. Shields, Nature (London) **501**, 69 (2013).
[8] S. Muralidharan, J. Kim, N. Lütkenhaus, M. D. Lukin, and L. Jiang, Phys. Rev. Lett. **112**, 250501 (2014).
[9] W. Zhang, D.-S. Ding, Y.-B. Sheng, L. Zhou, B.-S. Shi, and G.-C. Guo, Phys. Rev. Lett. **118**, 220501 (2017).
[10] Y. Xia, W. Li, W. Clark, D. Hart, Q. Zhuang, and Z. Zhang, Phys. Rev. Lett. **124**, 150502 (2020).
[11] J. I. Cirac, P. Zoller, H. J. Kimble, and H. Mabuchi, Phys. Rev. Lett. **78**, 3221 (1997).
[12] J. I. Cirac, A. K. Ekert, S. F. Huelga, and C. Macchiavello, Phys. Rev. A **59**, 4249 (1999).
[13] D. P. DiVincenzo, Fortschr. Phys. **48**, 771 (2000).
[14] S. Ritter, C. Nölleke, C. Hahn, A. Reiserer, A. Neuzner, M. Uphoff, M. Mücke, E. Figueroa, J. Bochmann, and G. Rempe, Nature (London) **484**, 195 (2012).
[15] I. A. Walmsley and J. Nunn, Phys. Rev. Appl. **6**, 040001 (2016).
[16] A. A. Clerk, M. H. Devoret, S. M. Girvin, F. Marquardt, and R. J. Schoelkopf, Rev. Mod. Phys. **82**, 1155 (2010).
[17] F. Ruesink, J. P. Mathew, M.-A. Miri, A. Alù, and E. Verhagen, Nat. Commun. **9**, 1798 (2018).
[18] J. P. Mathew, J. del Pino, and E. Verhagen, Nat. Nanotechnol. **15**, 198 (2020).

[19] Y. Chen, Y.-L. Zhang, Z. Shen, C.-L. Zou, G.-C. Guo, and C.-H. Dong, Phys. Rev. Lett. **126**, 123603 (2021).

[20] L. Fan, C.-L. Zou, R. Cheng, X. Guo, X. Han, Z. Gong, S. Wang, and H. X. Tang, Sci. Adv. **4**, eaar4994 (2018).

[21] R. Hisatomi, A. Osada, Y. Tabuchi, T. Ishikawa, A. Noguchi, R. Yamazaki, K. Usami, and Y. Nakamura, Phys. Rev. B **93**, 174427 (2016).

[22] R. W. Andrews, R. W. Peterson, T. P. Purdy, K. Cicak, R. W. Simmonds, C. A. Regal, and K. W. Lehnert, Nat. Phys. **10**, 321 (2014).

[23] I.-C. Hoi, C. M. Wilson, G. Johansson, T. Palomaki, B. Peropadre, and P. Delsing, Phys. Rev. Lett. **107**, 073601 (2011).

[24] K. Xia and J. Twamley, Phys. Rev. X **3**, 031013 (2013).

[25] I. Shomroni, S. Rosenblum, Y. Lovsky, O. Bechler, G. Guendelman, and B. Dayan, Science **345**, 903 (2014).

[26] Z. Wang, Y. Wu, Z. Bao, Y. Li, C. Ma, H. Wang, Y. Song, H. Zhang, and L. Duan, Phys. Rev. Appl. **15**, 014049 (2021).

[27] B. Vermersch, P.-O. Guimond, H. Pichler, and P. Zoller, Phys. Rev. Lett. **118**, 133601 (2017).

[28] C. T. Hann, C.-L. Zou, Y. Zhang, Y. Chu, R. J. Schoelkopf, S. M. Girvin, and L. Jiang, Phys. Rev. Lett. **123**, 250501 (2019).

[29] A. I. Lvovsky, B. C. Sanders, and W. Tittel, Nat. Photon. **3**, 706 (2009).

[30] C. L. Degen, F. Reinhard, and P. Cappellaro, Rev. Mod. Phys. **89**, 035002 (2017).

[31] W.-B. Yan and H. Fan, Sci. Rep. **4**, 4820 (2014).

[32] Y. T. Zhu and W. Z. Jia, Phys. Rev. A **99**, 063815 (2019).

[33] D.-C. Yang, M.-T. Cheng, X.-S. Ma, J. Xu, C. Zhu, and X.-S. Huang, Phys. Rev. A **98**, 063809 (2018).

[34] S. Weis, R. Rivière, S. Deléglise, E. Gavartin, O. Arcizet, A. Schliesser, and T. J. Kippenberg, Science **330**, 1520 (2010).

[35] C. Jiang, B. Chen, and K.-D. Zhu, J. Appl. Phys. **112**, 033113 (2012).

[36] G. S. Agarwal and S. Huang, Phys. Rev. A **85**, 021801(R) (2012).

[37] J.-T. Shen and S. Fan, Phys. Rev. Lett. **95**, 213001 (2005).

[38] L. Zhou, L.-P. Yang, Y. Li, and C. P. Sun, Phys. Rev. Lett. **111**, 103604 (2013).

[39] X. Li and L. F. Wei, Phys. Rev. A **92**, 063836 (2015).

[40] K. Xia, F. Jelezko, and J. Twamley, Phys. Rev. A **97**, 052315 (2018).

[41] M. Ahumada, P. A. Orellana, F. Domínguez-Adame, and A. V. Malyshev, Phys. Rev. A **99**, 033827 (2019).

[42] B. Poudyal and I. M. Mirza, Phys. Rev. Research **2**, 043048 (2020).

[43] D. Jalas *et al.*, Nat. Photon. **7**, 579 (2013).

[44] P. Lodahl, S. Mahmoodian, S. Stobbe, A. Rauschenbeutel, P. Schneeweiss, J. Volz, H. Pichler, and P. Zoller, Nature (London) **541**, 473 (2017).

[45] H. Jing, H. Lü, S. K. Özdemir, T. Carmon, and F. Nori, Optica **5**, 1424 (2018).

[46] R. Fleury, D. Sounas, and A. Alù, Nat. Commun. **6**, 5905 (2015).

[47] Y. Ma, H. Miao, B. H. Pang, M. Evans, C. Zhao, J. Harms, R. Schnabel, and Y. Chen, Nat. Phys. **13**, 776 (2017).

[48] L. Bi, J. Hu, P. Jiang, D. H. Kim, G. F. Dionne, L. C. Kimerling, and C. A. Ross, Nat. Photon. **5**, 758 (2011).

[49] C. Caloz, A. Alù, S. Tretyakov, D. Sounas, K. Achouri, and Z.-L. Deck-Léger, Phys. Rev. Appl. **10**, 047001 (2018).

[50] B. Peng, Ş. K. Özdemir, F. Lei, F. Monifi, M. Gianfreda, G. L. Long, S. Fan, F. Nori, C. M. Bender, and L. Yang, Nat. Phys. **10**, 394 (2014).

[51] L. Chang, X. Jiang, S. Hua, C. Yang, J. Wen, L. Jiang, G. Li, G. Wang, and M. Xiao, Nat. Photon. **8**, 524 (2014).

[52] A. B. Khanikaev and A. Alù, Nat. Photon. **9**, 359 (2015).

[53] J. Kim, M. C. Kuzyk, K. Han, H. Wang, and G. Bahl, Nat. Phys. **11**, 275 (2015).

[54] Z. Shen, Y.-L. Zhang, Y. Chen, C.-L. Zou, Y.-F. Xiao, X.-B. Zou, F.-W. Sun, G.-C. Guo, and C.-H. Dong, Nat. Photon. **10**, 657 (2016).

[55] S. Hua, J. Wen, X. Jiang, Q. Hua, L. Jiang, and M. Xiao, Nat. Commun. **7**, 13657 (2016).

[56] D. L. Sounas, J. Soric, and A. Alù, Nat. Electron. **1**, 113 (2018).

[57] Q.-T. Cao, R. Liu, H. Wang, Y.-K. Lu, C.-W. Qiu, S. Rotter, Q. Gong, and Y.-F. Xiao, Nat. Commun. **11**, 1136 (2020).

[58] Z. Yu and S. Fan, Nat. Photon. **3**, 91 (2009).

[59] N. A. Estep, D. L. Sounas, J. Soric, and A. Alù, Nat. Phys. **10**, 923 (2014).

[60] I. Söllner *et al.*, Nat. Nanotechnol. **10**, 775 (2015).

[61] S. Barzanjeh, M. Wulf, M. Peruzzo, M. Kalaee, P. B. Dieterle, O. Painter, and J. M. Fink, Nat. Commun. **8**, 953 (2017).

[62] K. Fang, J. Luo, A. Metelmann, M. H. Matheny, F. Marquardt, A. A. Clerk, and O. Painter, Nat. Phys. **13**, 465 (2017).

[63] S. A. R. Horsley, J.-H. Wu, M. Artoni, and G. C. La Rocca, Phys. Rev. Lett. **110**, 223602 (2013).

[64] S. Zhang, Y. Hu, G. Lin, Y. Niu, K. Xia, J. Gong, and S. Gong, Nat. Photon. **12**, 744 (2018).

[65] G. Lin, S. Zhang, Y. Hu, Y. Niu, J. Gong, and S. Gong, Phys. Rev. Lett. **123**, 033902 (2019).

[66] C. Liang, B. Liu, A.-N. Xu, X. Wen, C. Lu, K. Xia, M. K. Tey, Y.-C. Liu, and L. You, Phys. Rev. Lett. **125**, 123901 (2020).

[67] S. Maayani, R. Dahan, Y. Kligerman, E. Moses, A. U. Hassan, H. Jing, F. Nori, D. N. Christodoulides, and T. Carmon, Nature (London) **558**, 569 (2018).

[68] S. Barzanjeh, M. Aquilina, and A. Xuereb, Phys. Rev. Lett. **120**, 060601 (2018).

[69] R. Huang, A. Miranowicz, J.-Q. Liao, F. Nori, and H. Jing, Phys. Rev. Lett. **121**, 153601 (2018).

[70] G. A. Peterson, F. Lecocq, K. Cicak, R. W. Simmonds, J. Aumentado, and J. D. Teufel, Phys. Rev. X **7**, 031001 (2017).

[71] D. Malz, L. D. Tóth, N. R. Bernier, A. K. Feofanov, T. J. Kippenberg, and A. Nunnenkamp, Phys. Rev. Lett. **120**, 023601 (2018).

[72] K. Xia, G. Lu, G. Lin, Y. Cheng, Y. Niu, S. Gong, and J. Twamley, Phys. Rev. A **90**, 043802 (2014).

[73] K. Xia, F. Nori, and M. Xiao, Phys. Rev. Lett. **121**, 203602 (2018).

[74] M.-X. Dong, Y.-C. Yu, Y.-H. Ye, W.-H. Zhang, E.-Z. Li, L. Zeng, G.-C. Guo, D.-S. Ding, and B.-S. Shi, arXiv:1908.09242.

[75] M.-X. Dong, K.-Y. Xia, W.-H. Zhang, Y.-C. Yu, Y.-H. Ye, E.-Z. Li, L. Zeng, D.-S. Ding, B.-S. Shi, G.-C. Guo, and F. Nori, Sci. Adv. **7**, eabe8924 (2021).

[76] Y.-F. Jiao, S.-D. Zhang, Y.-L. Zhang, A. Miranowicz, L.-M. Kuang, and H. Jing, Phys. Rev. Lett. **125**, 143605 (2020).

[77] S. Klingler, H. Maier-Flaig, R. Gross, C.-M. Hu, H. Huebl, S. T. B. Goennenwein, and M. Weiler, Appl. Phys. Lett. **109**, 072402 (2016).
[78] N. Zhu, X. Han, C.-L. Zou, M. Xu, and H. X. Tang, Phys. Rev. A **101**, 043842 (2020).
[79] W. Yu, T. Yu, and G. E. W. Bauer, Phys. Rev. B **102**, 064416 (2020).
[80] X. Zhang, A. Galda, X. Han, D. Jin, and V. M. Vinokur, Phys. Rev. Appl. **13**, 044039 (2020).
[81] Y. Xu, J.-Y. Liu, W. Liu, and Y.-F. Xiao, Phys. Rev. A **103**, 053501 (2021).
[82] Y. Sun, W. Tan, H. Q. Li, J. Li, and H. Chen, Phys. Rev. Lett. **112**, 143903 (2014).
[83] D. Zhang, X.-Q. Luo, Y.-P. Wang, T.-F. Li, and J. Q. You, Nat. Commun. **8**, 1368 (2017).
[84] C. Wang, W. R. Sweeney, A. D. Stone, and L. Yang, Science **373**, 1261 (2021).
[85] C. H. Bennett and D. P. DiVincenzo, Nature (London) **404**, 247 (2000).
[86] K. Stannigel, P. Komar, S. J. M. Habraken, S. D. Bennett, M. D. Lukin, P. Zoller, and P. Rabl, Phys. Rev. Lett. **109**, 013603 (2012).
[87] T. Ramos, B. Vermersch, P. Hauke, H. Pichler, and P. Zoller, Phys. Rev. A **93**, 062104 (2016).
[88] S. Mahmoodian, P. Lodahl, and A. S. Sørensen, Phys. Rev. Lett. **117**, 240501 (2016).
[89] G. Hu, X. Hong, K. Wang, J. Wu, H.-X. Xu, W. Zhao, W. Liu, S. Zhang, F. Garcia-Vidal, B. Wang, P. Lu, and C.-W. Qiu, Nat. Photon. **13**, 467 (2019).
[90] A. Blais, J. Gambetta, A. Wallraff, D. I. Schuster, S. M. Girvin, M. H. Devoret, and R. J. Schoelkopf, Phys. Rev. A **75**, 032329 (2007).
[91] B. Peropadre, D. Zueco, F. Wulschner, F. Deppe, A. Marx, R. Gross, and J. J. García-Ripoll, Phys. Rev. B **87**, 134504 (2013).
[92] A. J. Sirois, M. A. Castellanos-Beltran, M. P. DeFeo, L. Ranzani, F. Lecocq, R. W. Simmonds, J. D. Teufel, and J. Aumentado, Appl. Phys. Lett. **106**, 172603 (2015).
[93] M. C. Collodo, A. Potočnik, S. Gasparinetti, J.-C. Besse, M. Pechal, M. Sameti, M. J. Hartmann, A. Wallraff, and C. Eichler, Phys. Rev. Lett. **122**, 183601 (2019).
[94] X. Zhang, C.-L. Zou, L. Jiang, and H. X. Tang, Phys. Rev. Lett. **113**, 156401 (2014).
[95] Y. Tabuchi, S. Ishino, T. Ishikawa, R. Yamazaki, K. Usami, and Y. Nakamura, Phys. Rev. Lett. **113**, 083603 (2014).
[96] D. Zhang, X.-M. Wang, T.-F. Li, X.-Q. Luo, W. Wu, F. Nori, and J. You, npj Quantum Inf. **1**, 15014 (2015).
[97] Y.-P. Wang, J. W. Rao, Y. Yang, P.-C. Xu, Y. S. Gui, B. M. Yao, J. Q. You, and C.-M. Hu, Phys. Rev. Lett. **123**, 127202 (2019).
[98] J.-T. Shen and S. Fan, Phys. Rev. A **82**, 021802(R) (2010).
[99] A. Megrant *et al.*, Appl. Phys. Lett. **100**, 113510 (2012).
[100] A. Romanenko, R. Pilipenko, S. Zorzetti, D. Frolov, M. Awida, S. Belomestnykh, S. Posen, and A. Grassellino, Phys. Rev. Appl. **13**, 034032 (2020).
[101] V. V. Konotop, J. Yang, and D. A. Zezyulin, Rev. Mod. Phys. **88**, 035002 (2016).